International Journal of Thermophysics, Vol. 23, No. 3, May 2002 (© 2002)

Non-Contact Measurements of Surface Tension and Viscosity of Niobium, Zirconium, and Titanium Using an Electrostatic Levitation Furnace

P.-F. Paradis,[1,2] T. Ishikawa,[1] and S. Yoda[1]

Received September 17, 2001

The surface tension and viscosity of liquid niobium, zirconium, and titanium have been determined by the oscillation drop technique using a vacuum electrostatic levitation furnace. These properties are reported over wide temperature ranges, covering both superheated and undercooled liquid. For niobium, the surface tension can be expressed as $\sigma(T) = 1.937 \times 10^3 - 0.199(T - T_m)$ (mN·m^{-1}) with $T_m = 2742$ K and the viscosity as $\eta(T) = 4.50 - 5.62 \times 10^{-3}(T - T_m)$ (mPa·s), over the 2320 to 2915 K temperature range. Similarly, over the 1800 to 2400 K temperature range, the surface tension of zirconium is represented as $\sigma(T) = 1.500 \times 10^3 - 0.111(T - T_m)$ (mN·m^{-1}) and the viscosity as $\eta(T) = 4.74 - 4.97 \times 10^{-3}(T - T_m)$ (mPa·s) where $T_m = 2128$ K. For titanium ($T_m = 1943$ K), these properties can be expressed, respectively, as $\sigma(T) = 1.557 \times 10^3 - 0.156(T - T_m)$ (mN·m^{-1}) and $\eta(T) = 4.42 - 6.67 \times 10^{-3}(T - T_m)$ (mPa·s) over the temperature range of 1750 to 2050 K.

KEY WORDS: niobium; noncontact processing; surface tension; titanium; viscosity; zirconium.

1. INTRODUCTION

The refractory nature and high resistance to chemical corrosion make metals such as niobium, zirconium, and titanium attractive for several applications [1]. Niobium and titanium have been primarily employed to harden alloys used in the automobile and aerospace industries, in particular, in the exhaust systems and in the hot section of aircraft gas turbine

[1] National Space Development Agency of Japan, Tsukuba Space Center, 2-1-1 Sengen, Tsukuba City, Ibaraki 305-8505, Japan.
[2] To whom correspondence should be addressed. E-mail: paradis.paulfrancois@nasda.go.jp

0195-928X/02/0500-0825/0 © 2002 Plenum Publishing Corporation

engines. In addition, niobium is used in arc-welding rods for stabilized grades of stainless steel, and, because of its superconducting properties, has been employed in making magnets. Due to its low neutron absorption cross section, zirconium is used in nuclear reactors. Titanium has been utilized in ship propeller shafts, rigging, and electrodes, and has potential use in desalination plants because of its excellent corrosion resistance to seawater.

Knowledge of the viscosity and the surface tension and their temperature dependences is paramount for various fundamental studies in atomic dynamics, surface physics, and related phenomena (Marangoni convection, etc.), as well as industrial processes such as bubble migration, refining, casting, and welding. These properties are also needed when designing new high performance alloys because the properties of an end member (e.g., binary, ternary systems, etc.) are required to estimate those of the final alloy. However, the high melting temperatures of these metals (Nb: 2742 K; Zr: 2128 K; Ti: 1943 K) and the risk of contamination at elevated temperatures make it very difficult to measure the thermophysical properties of their molten phases using traditional methods, in particular, surface tension, which is strongly affected by impurities. This motivated the use of sample levitation in vacuum and noncontact diagnostic techniques. The electrostatic levitation furnace constructed by the National Space Development Agency of Japan (NASDA) [2–5] circumvents the difficulties associated with high temperature processing and allows an accurate and quick determination of the thermophysical properties of different materials [6–9]. High temperature processing was achieved in vacuum by using multiple laser heating beams, thus isolating the sample from contaminating walls as well as surrounding gases and providing sufficient sample position stability for the thermophysical properties to be measured. The facility also permitted deep undercooling of the levitated sample, due to the containerless conditions and because sample heating and levitation were independent (electrostatic scheme does not input any heat). Also, since the sample was free from any enclosure, it represented an easy target for various diagnostics detectors and probes. In addition, the processing was done without inducing strong convection in the sample, which might cause premature nucleation in the melts [10].

Besides its use for thermophysical properties determination, this facility has a wide range of potential applications. For example, due to its containerless capabilities, it can be used to synthesize new materials, in particular, glass forming materials and alloys [11] with novel properties. Although its best feature lies in its ability to handle corrosive liquids, it is also attractive for the study of certain solids, such as niobium and molybdenum that exhibit corrosive activity at high temperature. A similar facility, currently under development, will be dedicated to the analysis of

the atomic structure of superheated and undercooled materials by neutron scattering experiments [12].

The present paper describes the electrostatic levitation facility and the method of determining the surface tension and viscosity, and presents the experimental results. The current work focuses on the surface tension and viscosity for overheated and undercooled niobium, zirconium, and titanium. Other thermophysical properties of these metals (liquid and solid phases), such as density, thermal expansion coefficient, constant pressure heat capacity, hemispherical total emissivity, and vapor pressure have already been reported elsewhere [6–9].

2. EXPERIMENTAL SETUP AND PROCEDURES

2.1. Electrostatic Levitation Furnace

The measurements reported in this paper have been carried out using an electrostatic levitation furnace constructed by NASDA [2–5]. Because Clancy et al. [13] proposed a concept for electrostatically positioning macroscopic bodies in space, the apparatus described here was based on the design by Rhim et al. [14] with modifications in areas of sample handling, charging, levitation initiation, imaging, and heating configuration [2–5, 15, 16], without which the described experiments would have been difficult to perform. Figure 1a illustrates schematically the electrostatic levitation furnace. The facility consists of a stainless steel chamber which was typically evacuated to $\sim 10^{-5}$ Pa before the sample processing was initiated. The chamber housed the sample that was levitated between two parallel disk electrodes, typically 10 mm apart. These electrodes (Fig. 1b) were used for vertical position sample control. The positioning system relied on a set of orthogonally disposed He-Ne lasers and the associated position detectors. The sample position information was fed to a computer that inputs new values of z to a high voltage amplifier at a rate of 720 Hz so that a prefixed position could be maintained. In addition, four spherical electrodes distributed around the bottom electrode were used for horizontal control, also via a feedback loop. The lower electrode was also surrounded by four coils, which generated a rotating magnetic field used for sample rotation control [17]. The top electrode was gimbaled by four micrometer screws, allowing accurate electrode balancing and spacing. The bottom electrode had a central hole that permitted sample handling. To excite drop oscillations, an ac voltage, superimposed on the levitation voltage, was inserted between the bottom electrode and the electric ground (Fig. 1a). A cartridge, with a 10-sample capacity, contained individual molybdenum pedestals, thus eliminating any cross contamination problems between

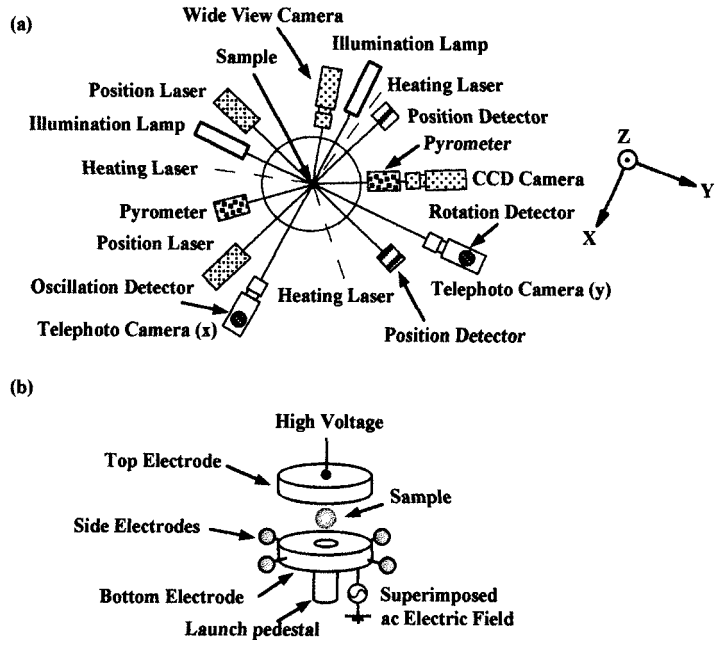

Fig. 1. Schematic view of NASDA—fs (a) electrostatic levitation furnace and (b) electrodes assembly.

different samples. For these experiments, the specimens were prepared by arc melting wire into spheroids with diameters ca 1.5 mm. The materials (Mo: 3N5; Nb: 2N5; Zr: 2N8; Ti: 3N) came from the Nilaco Corporation, Tokyo, Japan. A conical catcher was used to retrieve an unsuccessfully levitated sample.

The sample was observed by four charged-coupled-device (CCD) cameras. One camera offered a general view of both the electrode assembly and the sample. Another camera looked along the same path as a pyrometer to ensure constant alignment, to monitor the sample position in the horizontal plane, and to align the heating laser beams to minimize any detrimental photon pressure effects such as excessive rotation and oscillation on the levitated sample [18]. Control of rotation was of the utmost importance while measuring surface tension since a sample deformed by rotation could lead to erroneous data [19]. Two high resolution CCD cameras, equipped with telephoto objectives in conjunction with high intensity UV or visible background lights gave a close look at the sample, allowing sample perimeter and surface features to be analyzed [15]. In addition to the CCD cameras, each telephoto objective was equipped with a half-mirror, an interference filter (He-Ne emission line), and a detector.

To measure the sample oscillation using one of these detectors, the sample was backlit by a collimated He-Ne laser beam to generate a sample shadow on the detector. The shadow was masked from the detector except for a monochromator slit so that the detected signal was sensitive to the oscillating drop amplitude [20]. The other sensor allowed the sample rotation rate to be measured by detecting the reflected He-Ne laser beam from its surface [17].

Sample heating was performed using two 100 W CO_2 lasers (Synrad, Evolution 100) emitting at 10.6 μm. One beam was sent directly to the sample and the other beam was divided into two portions such that three focused beams, separated by 120 degrees, hit the specimen. Accurate computer control ensured that each beam delivered equal power to the sample. This configuration, together with maintaining a very low frequency rotation of the sample (< 5 Hz), ensured temperature homogeneity. Temperatures were measured over a 1250 to 3800 K range using two automatic pyrometers (Chino Corp, Model IR-CS 2S CG, operating at 0.90 μm and Chino Corp, Model IR-AP, operating at 0.96 μm) with respective acquisition rates of 10 and 120 Hz. The radiance temperature was measured by the pyrometers and was calibrated to true temperature using the known melting temperature of the materials. Calibration to true temperature was performed using a custom-made Code Warrior™ program, assuming that the set emissivity stayed constant over temperature.

To initiate levitation, the sample, in its launching position on the pedestal, was heated while monitoring its temperature with a pyrometer. The sample was heated with one beam whereas the two remaining beams converged at the location at which the sample was going to be positioned after the launch. Once the sample reached a temperature close to 1500 K, at which the thermionic emission was sufficient to charge the sample, the high voltage between the two electrodes was applied, and the feedback control software was activated. A few seconds later, the sample was launched into its normal levitation position. The preheating laser beam was then redirected on the sample to ensure position stability and to increase the temperature.

2.2. Surface Tension and Viscosity Measurements

The levitation furnace was particularly suitable to measure the surface tension and viscosity of superheated and undercooled liquids. Since sample heating and levitation were independent (electrostatic scheme does not input any heat), a precise laser heating control allowed undercooled melts to be maintained for time scales much longer than those required for measurements. Although no endurance test have been performed yet, it was

possible to maintain a 350 K undercooled and unperturbed Nb sample for more than 10 minutes. In addition, the spherical shape assumed by the levitated droplet (Fig. 2a) simplified the analysis compared to experiments with an electromagnetic levitator, when the oscillation drop technique was used [21].

The surface tension of liquid metals was determined by the oscillation drop technique, a method in which the frequency of the oscillation of levitated molten sample about its equilibrium shape was measured [20–26]. This method was attractive as it allowed measurements in the metastable state of undercooled melts and on highly reactive materials. This technique was described in detail [20] and is summarized below for completeness. To measure the surface tension using this method, a sample was first heated, became molten, and brought to a selected temperature, while closely ensuring excellent position stability, with no rotation and sample sphericity. Because the drop oscillation frequency and damping constant are affected by drop rotation (hence, surface tension and viscosity measurements), an exact knowledge of the sample rotation was imperative. However, the surfaces of the liquids processed in this study were so shiny that it was impossible to detect the rotation directly from the reflection of a He-Ne laser beam. Because the rotation is induced mainly through photon momentum transfer and since large laser power was required to melt the samples, rotation was visually detected (flattening of the sample along its equator) within a few minutes. As an added precaution, the samples were periodically solidified during the experiments so that the rotation rate could be measured accurately and the sample rotation stopped either with an applied magnetic field or by appropriately steering the laser beams. Once the sample was nonrotating, a $P_2\cos(\theta)$-mode drop oscillation was induced to the sample by superimposing a small sinusoidal electric field on the levitation field. Observation of the sample oscillation behavior on a TV monitor and the shape of the signal decay ensured that the correct oscillation mode was generated. Figure 2 shows side views of a levitated molten Nb sample before (a) and few milliseconds after the electrical excitation (b, c). The transient signal which followed the termination of the excitation field was detected and analyzed using a LabVIEW™ based, custom made program. The program reads the data that are assumed to follow the function,

$$y = Ae^{-t/\tau}\sin(\omega t + \phi) \tag{1}$$

where A is the amplitude, t is the time, τ is the decay time constant, ω is the frequency, and ϕ is a constant phase factor. The program then calculates values for the decay time constant and the frequency. Details about the

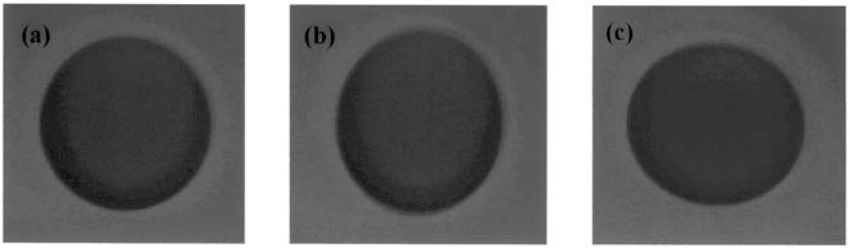

Fig. 2. Side view of a levitated molten Nb sample ($T = 2775$ K)(a) before and (b, c) after electrical excitation.

data analysis have already been reported [20]. A typical signal of the decay of the oscillation is shown in Fig. 3. The slight offset of the oscillation spectrum above the zero line can be accounted for by a tiny upward movement of the sample upon excitation. For a given sample at a selected temperature, up to 5 such signals were recorded and this was repeated at different temperatures (3 to 10, depending on material). For a given material, the measurements were made on several samples. At the time the oscillation frequency was measured, the rotation rate of the sample was well below 10 Hz. From a paper by Rhim and Ishikawa [19], it is inferred that the estimated errors on the final results due to residual rotation should be negligible. Using the characteristic oscillation frequency ω_c of this signal after correcting for nonuniform surface charge distribution [27], the surface tension σ could be found from the following equation [21, 26],

$$\omega_c^2 = (8\sigma/r_0^3\rho)[1-(Q^2/64\pi^2 r_0^3\sigma\varepsilon_0)][1-F(\sigma, q, e)] \tag{2}$$

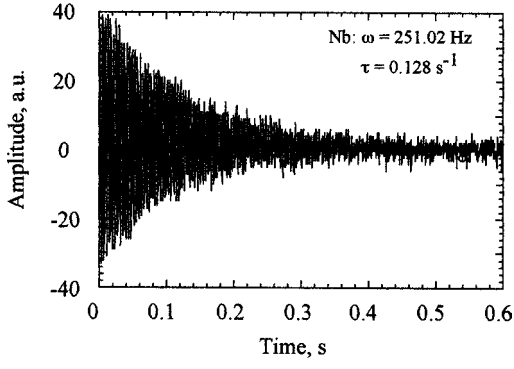

Fig. 3. Typical signal of the decay of the oscillation following electrical excitation, shown for Nb.

where

$$F(\sigma, q, e) = [243.31\sigma^2 - 63.14q^2\sigma + 1.54q^4]\, e^2/[176\sigma^3 - 120q^2\sigma^2 + 27\sigma q^4 - 2q^6] \tag{3}$$

and r_0 is the radius of the sample when it assumed a spherical shape, ρ is the liquid density, Q is the drop charge, ε_0 is the permittivity of vacuum, and q and e are defined by

$$q^2 = Q^2/16\pi^2 r_0^3 \varepsilon_0 \tag{4}$$

and

$$e^2 = E^2 r_0 \varepsilon_0 \tag{5}$$

respectively, with E being the applied electric field. Similarly, using the decay time τ given by the same signal, the viscosity η was found by

$$\eta = \rho r_0^2/5\tau \tag{6}$$

From Eqs. (2) and (6), it can be seen that both the surface tension and the viscosity depend on the sample radius and density. For density, we simply substituted our previously determined data in these equations [6–8]. Also, to ensure that the measured properties were not distorted by sample evaporation, it was decided to monitor the radius variation in real time using the imaging technique described earlier [15] instead of relying solely on a measurement of the mass of the sample before and after the experiment, as done elsewhere [20, 28]. Hence, a real-time value of the radius was used. A forthcoming paper will explain this procedure in details, showing in particular how it can be applied to measure the vapor pressure of high-temperature liquid materials [9].

EXPERIMENTAL RESULTS

Previous experiments with tin samples showed that patches of oxides floating on a liquid sample could be easily detected either visually with telephoto cameras or with our He-Ne laser based sample rotation detection system. Although some traces of oxidation were observed on solid samples prior to melting in the present experiments, these unstable oxides were easy

to break and were neither tracked by the rotation detection nor by visual observation when the samples were liquefied. The samples very shiny after processing, showed no signs of oxidation during solidification.

In this study, due to the large laser power required to melt the samples, the choice in sample diameter was very limited. Therefore, the diameters of samples of a same material were similar. However, in an early stage of implementing the oscillation method, a study with Sn showed that a change in diameter (in the 1.5 to 2.5 mm range) did not induce any change in the property measurements.

3.1. Surface Tension

Our results for the surface tension measurements are plotted in Fig. 4. The surface tension of niobium, zirconium, and titanium, as observed for other pure metals, exhibited a linear dependence on temperature. In these experiments, the uncertainty of the measurements was estimated to be better than 5% from the uncertainty associated with each parameter of Eq. (2). The uncertainty on the frequency was related with the response of the oscillation detector, that of the electrical charge with the resolution of the voltage amplifier, and those of the radius and density with the resolution of the video grabbing capabilities (640×480 pixels) and from the uncertainty in mass measurement (± 0.0001 g). The data available from the literature were also superimposed on the same figure for comparison. In addition, Table I summarizes existing surface tension data with the corresponding temperature range of applicability and the measurement technique.

3.1.1. Niobium

The surface tension of niobium (Fig. 4a), measured over the 2320 to 2915 K temperature range and covering the undercooled region for more than 400 K, can be expressed by

$$\sigma(T) = 1.937 \times 10^3 - 0.199(T - T_m)\ (\mathrm{mN \cdot m^{-1}})\ (2320 \text{ to } 2915\ \mathrm{K}) \qquad (7)$$

where T_m is the melting temperature (2742 K). These measurements were the first to cover a large temperature range. At the melting temperature, our result was systematically higher than the values that were determined with the pendant drop technique. It was less than 2% higher than that obtained by Allen [29] and within 6% with those reported by Flint [30] and Ivaschenko and Marchenuk [31]. Our temperature coefficient was however nearly 17% lower than that calculated by Allen [29].

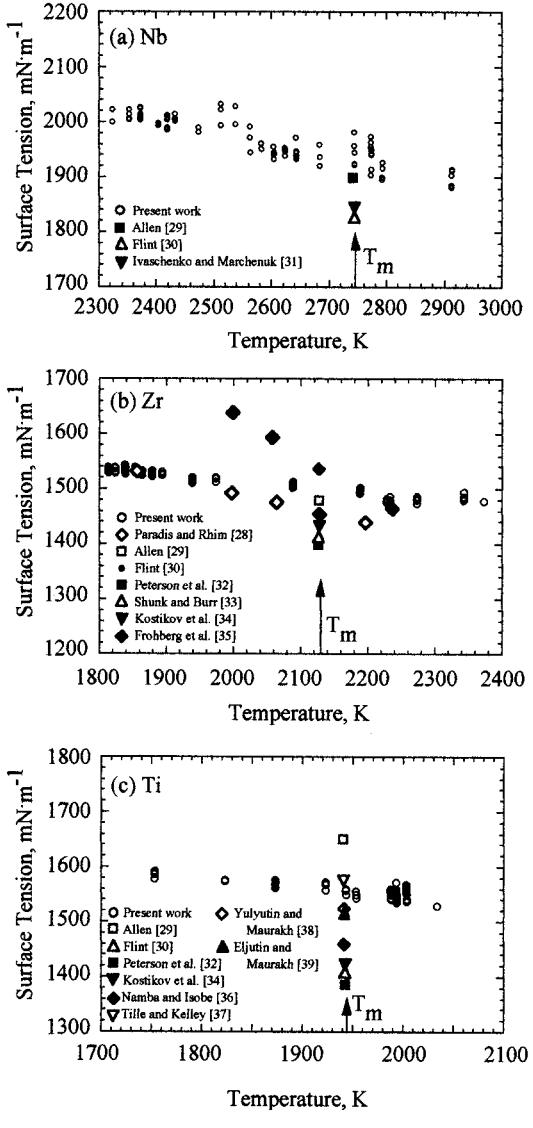

Fig. 4. Surface tension versus temperature: (a) Nb; (b) Zr; (c) Ti.

Table I. Literature Values for the Surface Tension of Nb, Zr, and Ti

Element	Surface Tension ($mN \cdot m^{-1}$)	Temp. Coeff. (K^{-1})	Temperature (K)	Reference	Technique
Nb	1937	−0.199	2320–2915	present work	levitation
	1900	−0.24	2742	[29]	pendant drop
	1827	—	2742	[30]	pendant drop
	1840	—	2742	[31]	pendant drop
Zr	1500	−0.111	1800–2400	present work	levitation
	1459	−0.244	1850–2200	[28]	levitation
	1480	−0.20	2128	[29]	pendant drop
	1457	—	2128	[30]	pendant drop
	1400	—	2128	[32]	drop weight
	1411	—	2128	[33]	drop weight
	1430	—	2128	[34]	pendant drop
	1543	−0.66	2000–2250	[35]	levitation
Ti	1557	−0.156	1750–2050	present work	levitation
	1650	−0.26	1943	[29]	pendant drop
	1402	—	1943	[30]	pendant drop
	1390	—	1943	[32]	pendant drop
	1410	—	1943	[34]	pendant drop
	1460	—	1943	[36]	drop weight
	1576	—	1943	[37]	drop weight
	1510	—	1943	[38]	drop
	1510	—	1943	[39]	capillary

3.1.2. Zirconium

For zirconium (Fig. 4b), the surface tension was measured over the 1800 to 2400 K temperature range that included the undercooled region for more than 320 K and was fitted by

$$\sigma(T) = 1.500 \times 10^3 - 0.111(T - T_m)\ (mN \cdot m^{-1})\ (1800 \text{ to } 2400\ K) \qquad (8)$$

At the melting temperature ($T_m = 2128$ K), our result was generally higher than those found in the literature, being, respectively, 1.3 and 3% higher than those reported by Allen [29] and Flint [30]. It was also 7% higher compared with those of Peterson et al. [32] and Shunk and Burr [33] obtained with the drop weight technique. Our measurement was 5% larger than the value determined by Kostikov et al. [34] using a pendant drop technique and agreed within 2.8% with that measured by Paradis and Rhim [28] with an electrostatic levitator. However, our value was lower by 2.8% than that obtained by Frohberg et al. [35] with electromagnetic levitation. Our temperature coefficient was close to 44.5% lower than that

calculated by Allen [29], 54.5% smaller than that determined by Paradis and Rhim [28], and a factor of six lower than that reported by Frohberg et al. [35].

3.1.3. Titanium

Due the high vapor pressure of titanium, particular care was taken to maintain clean viewing ports, in particular, that of the pyrometer when measuring the surface tension (Fig. 4c). The presented data cover a wide temperature range (1750 to 2050 K) including the undercooled region for nearly 200 K and can be represented by

$$\sigma(T) = 1.557 \times 10^3 - 0.156(T - T_m)\ (\mathrm{mN \cdot m^{-1}})\ (1750 \text{ to } 2050\ \mathrm{K}) \qquad (9)$$

where T_m is the melting temperature (1943 K). Although several values have been published in the literature at the melting point, we believe that our measurements are the first to cover a large temperature range. At the melting temperature, our value agreed within 5.6% with that obtained by Allen [29], to within 11% with that measured by Flint [30], to within 12% with that reported by Peterson et al. [32], and to within 10.4% with that given by Kostikov et al. [34]. Our result was 6.6% lower than that of Namba and Isobe [36], agreed within mutual experimental uncertainties, to that reported by Tille and Kelly [37], was 3.1% higher than that published by Yulyutin and Maurakh [38], and agreed within 3.1% with that measured by Eljutin and Maurakh [39]. Our temperature coefficient was nearly 40% smaller than that calculated by Allen [29].

3.2. Viscosity

By extracting the decay time components from the decay of the oscillation of a sample used to measure surface tension (Fig. 3), it was possible to determine the viscosity of a metal over the same temperature range. Figure 5 shows that the viscosity of these elements exhibits a linear dependence with temperature, as is the case for other pure metals. Superimposed on the graphs are data found in the literature. The data are further summarized in Table II and compared with those reported in the literature. The viscosity data scatter can be explained by the decay constant alteration due to slight sample upward motions that occurred when the oscillation was initiated. Within the scatter, the results were nonetheless reproducible whichever batch of samples we used.

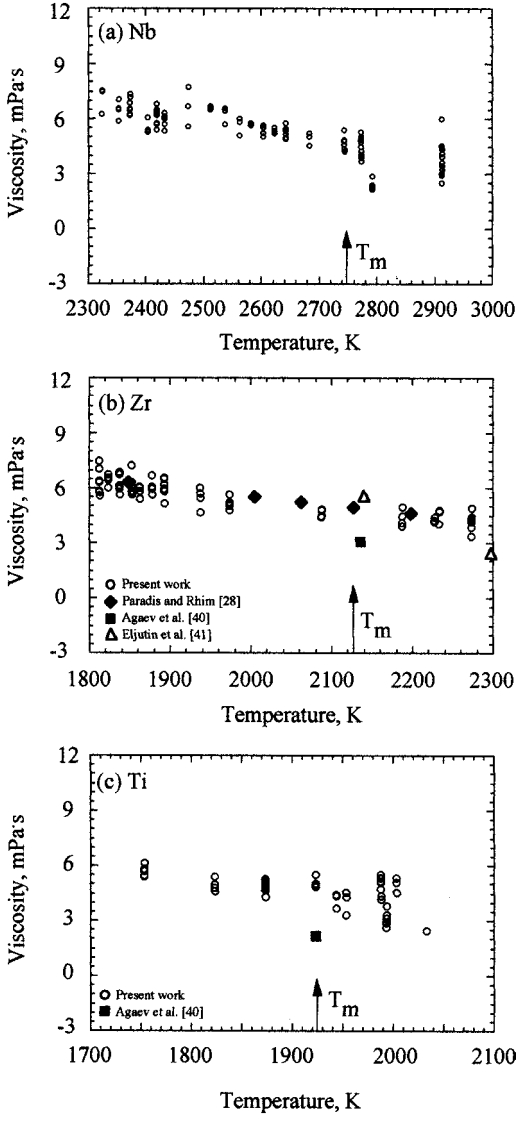

Fig. 5. Viscosity versus temperature: (a) Nb; (b) Zr; (c) Ti.

Table II. Literature Values for the Viscosity of Nb, Zr, and Ti

Element	Viscosity (mPa⁻s)	Temp. Coeff. (K^{-1})	Temperature (K)	Reference	Technique
Nb	4.50	−0.00562	2320–2915	present work	levitation
Zr	4.74	−0.00497	1800–2300	present work	levitation
	4.83	−0.00531	1850–2200	[28]	levitation
	3.5	—	2133	[40]	capillary
	5.45	—	2138	[41]	capillary
	2.4	—	2300	[41]	capillary
Ti	4.42	−0.00667	1750–2050	present work	levitation
	2.2	—	1943	[40]	capillary

3.2.1. Niobium

The temperature dependence of the viscosity of overheated and undercooled niobium is illustrated in Fig. 5b over the 2320 to 2915 K range. The data could be fitted by the following equation:

$$\eta(T) = 4.50 - 5.62 \times 10^{-3}(T - T_m)\ (\text{mPa} \cdot \text{s})\ (2320 \text{ to } 2915 \text{ K}) \qquad (10)$$

where T_m is the melting temperature (2742 K). No other data for niobium could be found. The value obtained has, however, the same order of magnitude as those reported for other refractory metals (e.g., Zr, Ti, etc.) (Table II).

3.2.2. Zirconium

For zirconium, the viscosity (Fig. 5c) was measured over the 1800 to 2300 K temperature range that includes the undercooled region for more than 320 K. It can be expressed as

$$\eta(T) = 4.74 - 4.97 \times 10^{-3}(T - T_m)\ (\text{mPa} \cdot \text{s})\ (1800 \text{ to } 2300 \text{ K}) \qquad (11)$$

where T_m is the melting temperature (2128 K). The few values that appear in the literature at various temperatures are summarized in Table II. At the corresponding temperature, our result is 35% higher than that measured by Agaev et al. [40] (2133 K) with the capillary technique. Also, our values were, respectively, 13% lower (2138 K) and close to a factor of two larger (2300 K) than those obtained by Eljutin et al. [41] with the capillary method. At the melting temperature, our value was 1.9% smaller and our temperature coefficient was 6.4% smaller than those measured by Paradis and Rhim with an electrostatic levitation system [28].

3.2.3. *Titanium*

Viscosity data for titanium (Fig. 5d) were obtained over a wide temperature range (1750 to 2050 K) that covered the undercooled region for almost 200 K. A linear fit yielded

$$\eta(T) = 4.42 - 6.67 \times 10^{-3}(T - T_m)\ (\text{mPa} \cdot \text{s})\ (1750 \text{ to } 2050\ \text{K}) \qquad (12)$$

We believe that these measurements are the first to be reported for titanium that include a large temperature range. At the melting temperature ($T_m = 1943$ K), our value was about a factor of two larger than that reported by Agaev et al. [40] using the capillary technique, the only other result found in the literature.

4. DISCUSSION

The discrepancies between our results and those reported by other investigators [29–34, 36–41] could be attributed to differences in processing techniques. In this work, containerless levitation in vacuum and radiative heating isolated the samples from container walls and gases, whereas the above authors employed the pendant drop or drop weight methods for which possible chemical reactions between the highly reactive molten metals and residual gas or gaseous atmospheres could have altered the final surface tension or viscosity values, which are highly dependent upon contamination. According to Keene [42], very small amounts (monolayers) of oxygen can decrease the surface tension of metals by as much as 50%. This may explain why our values are generally higher than those obtained with classical, non-levitation techniques. In addition, electron bombardment and induction heating, used by the above authors, might have been accompanied with some evaporation from the electrodes or from the heating elements, thus further contaminating the specimens under study. This might also explain why our results for surface tension were generally higher than those obtained with noncontainerless techniques for niobium and zirconium. Because titanium has a high vapor pressure, self-cleaning of the surface might have prevented, to some extent, contamination.

Although performing property measurements with a levitated sample has many advantages, some specific errors to levitation occur in the measurement process because the sample sometimes moves along the three axes, oscillates, or evaporates (diameter changes in time) thus contributing to discrepancies. The problem is more severe with refractory metals since their high melting temperature requires large laser powers that favor photon momentum transfer. To explain the difference between our results

and those obtained by Frohberg et al. [35] with an electromagnetic containerless facility, we refer to a paper by Chen and Overfelt [43] who pointed out that the magnetic field used in these levitators causes a slight increase in the stiffness of the drop, raising the apparent surface tension. This effect may be more pronounced for the large samples they used because the specimens feel a stronger magnetic pressure. Purity in the samples and level of vacuum could also explain, to some extent, the discrepancies between our data and those obtained by other investigators using containerless techniques [28, 35]. Although Paradis and Rhim [28] also carried out measurements in vacuum using an electrostatic levitation furnace and laser heating, the small discrepancies observed between the two data sets could be explained by the fact that we carefully kept track of the change of the sample radius in the current study.

5. CONCLUSIONS

The surface tension and viscosity of superheated and undercooled niobium, zirconium, and titanium have been measured over large temperature ranges. The surface tension and viscosity data presented in this paper were obtained from analysis of the induced sample oscillations coupled with an imaging technique to monitor the sample radius variation during the whole processing duration. Therefore, to improve the data, efforts are being focused towards ways to improve signal acquisition and amplification, and techniques to increase image sharpness. Current activities are also directed on the measurements of surface tension and viscosity of other refractory metals such as molybdenum, tantalum, rhenium, and tungsten in their superheated and undercooled states. Also, there are hopes that modification of the measurement techniques could be applied to low viscosity dielectric oxide ceramic and glass forming materials in conjunction with the novel hybrid electrostatic-aerodynamic levitation furnace recently by our laboratory [44].

During the experiments, extreme care was taken to keep the sample in a fixed position during the excitation and the observation of the following decay to ensure constant heating. Although previous experiments showed that samples could be maintained in their deeply undercooled states for periods exceeding 10 minutes, it was observed, under otherwise identical situations, that an excited undercooled sample is more prone to premature nucleation when an excitation field was applied. Experiments are presently planned to investigate this phenomenon and to see whether the excitation field itself or the resulting surface change (that modifies the surface energy) might lower the energy potential barrier required for nucleation. Experiments and analysis on that important issue and its implication to justify

materials processing in microgravity will be addressed in a forthcoming article.

ACKNOWLEDGMENTS

The authors would like to acknowledge Dr. J. Yu for his careful reading of the manuscript. Thanks are extended to Dr. Aoyama for help in some experiments and to Dr. Y. Arai and Dr. N. Koshikawa for discussions.

REFERENCES

1. D. R. Lide and H. P. R. Frederikse (eds.), *CRC Handbook of Chemistry and Physics*, 78th ed. (CRC Press, Boca Raton, Florida, 1997).
2. P.-F. Paradis, T. Ishikawa, and S. Yoda, in *Proc. Spacebound 2000*, Vancouver, Canada, May 2000 (Canadian Space Agency, 2001).
3. P.-F. Paradis, T. Ishikawa, and S. Yoda, in *Proc. First Int. Symp. Microgravity Res. Applications in Phys. Sci. and Biotech.*, Sorrento, Italy, September 2000 (ESA SP-454, 2001), p. 993.
4. T. Ishikawa, P.-F. Paradis, and S. Yoda, *J. Jpn. Soc. Microg. Appl.* **17**:98 (2000).
5. T. Ishikawa, P.-F. Paradis, and S. Yoda, *J. Jpn. Soc. Microg. Appl.* **18**:106 (2001).
6. T. Ishikawa, P.-F. Paradis, and S. Yoda, *2nd Pan-Pacific Basin Workshop on Microgravity Sciences*, TP-1019, Pasadena, California, in press.
7. P.-F. Paradis, T. Ishikawa, and S. Yoda, *J. Mater. Sci.* **36**:5125 (2001).
8. P.-F. Paradis, T. Ishikawa, and S. Yoda, *Int. J. Thermophys.* **23**:(2002).
9. P.-F. Paradis, T. Ishikawa, and S. Yoda, to be submitted to *Rev. Sci. Instrum.*
10. C. S. Ray and D. E. Day, *2nd AIAA 40th Aerospace Sciences Meeting and Exhibit,* AIAA-2002-0768, Reno, Nevada, in press.
11. J. Yu, P.-F. Paradis, T. Ishikawa, S. Ozawa, T. Saito, T. Motegi, and S. Yoda, *Japan. J. Appl. Phys.*, in press.
12. P.-F. Paradis, T. Ishikawa, and S. Yoda, *Proc. of the LAM 11 Conf. (J. Non-Cryst. Solids)*, Yokohama, Japan, Sept. 2001, in press.
13. P. F. Clancy, E. G. Lierke, R. Grossbach, and W. M. Heide, *Acta Astron.* **7**:877 (1980).
14. W.-K. Rhim, S.-K. Chung, D. Barber, K.-F. Man, G. Gutt, A. A. Rulison, and R. E. Spjut, *Rev. Sci. Instrum.* **64**:2961 (1993).
15. T. Ishikawa, P.-F. Paradis, and S. Yoda, *Rev. Sci. Instrum.* **72**:2490 (2001).
16. P.-F. Paradis, T. Ishikawa, and S. Yoda, to be submitted to *Space Technol.*
17. W.-K. Rhim and T. Ishikawa, *Rev. Sci. Instrum.* **69**:3628 (1998).
18. W.-K. Rhim and P.-F. Paradis, *Rev. Sci. Instrum.* **70**:4652 (1999).
19. W.-K. Rhim and T. Ishikawa, *Rev. Sci. Instrum.*, in press.
20. W.-K. Rhim, K. Ohsaka, P.-F. Paradis, and R. E. Spjut, *Rev. Sci. Instrum.* **70**:2796 (1999).
21. S. Sauerland, G. Lohofer, and I. Egry, *J. Non Cryst. Solids* **156–158**:833 (1993).
22. Lord Rayleigh, *Proc. R. Soc. London.* **14**:184 (1882).
23. M. E. Fraser, W.-K. Lu, A. E. Hamielec, and R. Murarka, *Metall. Trans.* **2**:817 (1971).
24. H. Soda, A. McLean, and W.A. Miller, *Metall. Trans. B* **9**:145 (1978).
25. B.J. Keene, K. C. Mills, A. Kasama, A. McLean, and W. A. Miller, *Metall. Trans. B* **17**:159 (1986).
26. I. Egry and J. Szekely, *Adv. Space Res.* **11**:263 (1991).

27. J. Q. Feng and K. V. Beard, *Proc. R. Soc. London A* **430**:133 (1990).
28. P.-F. Paradis and W.-K. Rhim, *J. Mater. Res.* **14**:3713 (1999).
29. B. C. Allen, *Trans. AIME* **227**:1175 (1963).
30. O. Flint, *J. Nucl. Mat.* **16**:260 (1965).
31. Yu. N. Ivaschenko and P. C. Marchenuk, *Teplov. Vys. Temp. (USSR)* **11**:1285 (1973).
32. A. W. Peterson, H. Kedesdy, P. H. Keck, and E. Scharz, *J. Appl. Phys.* **28**: 213 (1958).
33. R. Shunk and M. Burr, *Trans. AIME* **55**:786 (1962).
34. V. I. Kostikov, B. D. Grigorjev, P. G. Arkhipkin, and A. D. Agaev, *Izv. Vyss. Uch. Sav. Chern. Met. (USSR)* **3**:25 (1972).
35. M. G. Frohberg, M. Roesner-Kuhn, and G. Kuppermann, in *Int. Workshop on Nucleation and Thermophys. Props. of Undercooled Melts*, Phyzikzentrum Bad Honnef, March 4–6, 1998.
36. S. Namba and T. Isobe, *Sci. Pap. Inst. Phys. Chem. Res., Tokyo*. **57**:5154 (1963).
37. S. Tille and R. Kelly, *Br. J. Appl. Phys.* **146**:717 (1963).
38. V. P. Yulyutin and M. Maurakh, *Izvest. Akad. Nauk. (USSS)* **4**:129 (1956).
39. V. P. Eljutin and M. A. Maurakh, *Izv. A.N., O.T.N. (USSR)* **4**:29 (1956).
40. A. D. Agaev, V. I. Kostikov, and V. N. Bobkovskii, *Izv. Akad. Nauk. SSSR Met.* **3**:43 (1980).
41. V. P. Eljutin, M. A. Maurakh, and V. D. Turov, *Izv. Vyssh. Ucheb. Zaved. Chem. Met. (USSR)* **8**:110 (1965).
42. B. J. Keene, *Surface Tension of Pure Metals*, National Physical Laboratory, Publication DMM(A) 39 (1991).
43. S.-F. Chen and R.A. Overfelt, *Int. J. Thermophys.* **19**:817 (1998).
44. P.-F. Paradis, T. Ishikawa, J. Yu, and S. Yoda, *Rev. Sci. Instrum.* **72**:2811 (2001).